

Dynamics of two interacting electrons in Anderson-Hubbard chains with long-range correlated disorder: Effect of a static electric field

W. S. Dias, E. M. Nascimento, M. L. Lyra, and F. A. B. F. de Moura
Instituto de Física, Universidade Federal de Alagoas, 57072-970 Maceió, AL, Brazil
 (Received 19 November 2009; published 13 January 2010)

We investigate the influence of the on-site Hubbard interaction U on the eigenstates and dynamics of two electrons restricted to move in a linear chain with long-range correlated disorder. We solve the time-dependent Schrödinger equation to follow the time evolution of an initially localized Gaussian two-electron wave packet. In the regime of strongly correlated disorder, for which one-electron extended eigenstates emerge near the band center, the electron-electron coupling promotes the trapping of a finite portion of the wave packet. In the presence of a uniform electric field, the wave packet develops complex Bloch oscillations. The power spectrum of the centroid's velocity trace shows a splitting near the typical semiclassical Bloch frequency, as well as a frequency doubling phenomenon for intermediate couplings which is related to the bounded states components that are present in the wave packet. Finally, we show that localized and extended two-electron eigenstates coexist near the band center with the level spacing distribution showing a universal Poissonian form irrespective to the Hubbard coupling.

DOI: [10.1103/PhysRevB.81.045116](https://doi.org/10.1103/PhysRevB.81.045116)

PACS number(s): 71.10.Li, 73.20.At, 71.20.-b, 05.60.Gg

I. INTRODUCTION

The time evolution of one-electron wave packets in low-dimensional disordered systems is a well-known problem with several connections with transport phenomena.¹ For low-dimensional systems with uncorrelated disorder, the Anderson localization theory predicts the absence of extended eigenstates.¹⁻³ This means that the width of the time-dependent wave packet saturates in the long-time limit, i.e., the electron remains localized in a finite region around the initial position. The presence of short- or long-range correlations in the disorder distribution is a key mechanism to induce extended states in the one-dimensional (1D) Anderson model.⁴⁻¹⁰ In fact, it has been established that short-range correlated on-site disorder may lead to the appearance of extended states at special resonance energies.⁴⁻⁶ However, these states form a set of null measure of the density of states in the thermodynamic limit, which implies in the absence of mobility edges in such models.

On the other hand, long-range correlations can induce a metal-insulator transition in 1D systems.⁸⁻¹⁰ A strategy to achieve this is to consider a 1D system with nearest-neighbor hopping integrals and a long-range correlated on-site disorder distribution with a powerlike spectrum behaving as $k^{-\alpha}$. Whenever the standard deviation of the energy distribution is equal to the nearest-neighbor hopping and $\alpha < 2$, all states remain localized and the Lyapunov exponent is finite on the entire energy band. For $\alpha > 2$, a phase of extended states appears at the center of the energy band, giving rise to two mobility edges. After this finding, models with long-range correlated on-site disorder distributions have attracted much attention. Scaling properties of the localization length¹¹ and local density of states¹² close to the critical point have been subjects of recent studies. Further, the metal-insulator transition in the two-dimensional Anderson model with long-range correlations was characterized by measuring the participation number exponent from the long-time behavior of the wavefunction spacial distribution.¹³ The theoretical prediction of

delocalization induced by correlated disorder has been confirmed by experimental works in semiconductor superlattices¹⁴ and microwave transmission spectra through a single-mode waveguide with correlated scatterers.¹⁵ Several works suggest that an appropriate algorithm for generating random correlated sequences with desired mobility edges could be used in the manufacture of filters for electronic or optical signals.⁹

A key problem in condensed-matter physics is to understand the electronic transport when disorder, interaction, and electric field effects are simultaneously present. The interplay between disorder and dynamical localization due to an electric field was recently studied in Refs. 16 and 17. It was numerically shown that coherent Bloch oscillations can appear whenever the disorder distribution displays appropriated long-range correlations in both one-dimensional¹⁶ and two-dimensional¹⁷ systems. The problem involving disorder and electron-electron interaction has been a subject of great interest due to their competitive roles.¹⁸⁻³¹ It has been shown that an on-site Hubbard interaction weakens the Anderson localization induced by disorder. Shepelyansky¹⁸ pioneered the study of two interacting electrons moving in a disordered 1D system and obtained an enhanced propagation effect of an interacting electron pair over distances larger than the single-particle localization length, as indeed predicted in disordered mesoscopic rings threaded by a magnetic flux.²⁰ Recently, the interplay between dynamical localization and electron-electron interaction was reported in Refs. 32-35. By using numerical and analytical calculations, the problem involving N interacting electrons moving along a chain and subject to an external electric field was studied in Ref. 32. It was shown that the N -particle problem is identical to that of a single-particle moving in an N -dimensional lattice, with defect surfaces dividing the space in symmetric domains. It was shown that in the limit of a weak hopping integral, the electron-electron interaction induces an additional oscillation of the eigenstates drift velocity. The period of this oscillation was found to be determined solely by the range and strength

of the electron-electron interaction.³² By using an extended dynamical mean-field theory,³⁴ the effect of a large electric field on interacting electrons was studied, numerically demonstrating that the Bloch oscillations decay due to electron correlations.

In this work, we provide a detailed analysis of the interplay between electron-electron interaction, correlated disorder, and an external field using a prototype one-dimensional tight-binding Anderson-Hubbard Hamiltonian to describe a two-electron system. To this end, we focus on the electric field biased wave-packet dynamics of two interacting electrons moving in a 1D chain with long-range correlated disorder. We build a disordered long-range correlated on-site energy distribution using the formalism introduced in Refs. 8 and 10 which generates a random sequence with power spectrum proportional to $1/k^\alpha$, where k is the wave vector of the modulations on the random sequence landscape. We will use numerical methods to solve the Schrödinger equation and compute the stationary eigenstates and the time evolution of the two-electron wave packet. Starting from an initial Gaussian wave packet, we will be mainly interested in revealing the hole played by the bounded two-electron states generated by the Hubbard-type coupling in the biased and unbiased wave-packet dynamics, particularly in the regime of strongly correlated disorder for which a band of extended states is expected to emerge. Finally, we will also compute the level spacing distribution and discuss its dependence on the electron-electron coupling under the light of the usual random matrix results for disordered one-electron systems.

II. MODEL AND FORMALISM

The Anderson-Hubbard tight-binding Hamiltonian for two interacting electrons moving in a 1D system with correlated disorder in the presence of a static uniform electric field F is given by^{30,31}

$$H = \sum_n \sum_s W(c_{n+1,s}^\dagger c_{n,s} + c_{n,s}^\dagger c_{n+1,s}) + \sum_n \sum_s [\epsilon_n + eFan] c_{n,s}^\dagger c_{n,s} + \sum_n U c_{n,\uparrow}^\dagger c_{n,\uparrow} c_{n,\downarrow}^\dagger c_{n,\downarrow}, \quad (1)$$

where $c_{n,s}$ and $c_{n,s}^\dagger$ are the annihilation and creation operators for the electron at site n with spin s , \mathbf{n} is the position operator, W is the hopping amplitude, U is the on-site Hubbard electron-electron interaction, and e is the electron charge. In order to introduce long-range correlations in the disorder distribution, the sequence of site energies obeys the relation^{8,10}

$$\epsilon_n = \zeta(\alpha, N) \sum_{k=1}^{N/2} \left(\frac{1}{k}\right)^{\alpha/2} \cos\left(\frac{2\pi nk}{N} + \phi_k\right), \quad (2)$$

where $\{\phi_k\}$ are $N/2$ independent random phases uniformly distributed in the interval $[0, 2\pi]$. This energy sequence is shifted in order to have $\langle \epsilon_n \rangle = 0$. $\zeta(\alpha, N)$ is used to set the energy sequence variance $\Delta \epsilon_n = 1$ for all system sizes. The parameter α controls the degree of correlations. In the absence of an external field and in the limit of noninteracting

electrons, this model presents a band of extended states for $\alpha > 2$.⁸

A. Time-dependent Schrödinger equation analysis

In order to follow the time evolution of two-electron wave packets, we solve the time-dependent Schrödinger equation by expanding the wave function in the Wannier representation

$$|\Phi(t)\rangle = \sum_{n_1, n_2} f_{n_1, n_2}(t) |n_1 s_1, n_2 s_2\rangle, \quad (3)$$

where the ket $|n_1 s_1, n_2 s_2\rangle$ represents a state with one electron with spin s_1 at site n_1 and the other electron with spin s_2 at site n_2 . To allow for double occupancy of the on-site orbitals, we will consider in the following that the electrons are in distinct spin states (singlet state). Once the initial state is prepared as a direct product of states, the electrons will always be distinguishable by their spins since the Hamiltonian does not involve spin-exchange interactions. The time evolution of the wave function in the Wannier representation becomes

$$i \frac{df_{n_1, n_2}(t)}{dt} = f_{n_1+1, n_2}(t) + f_{n_1-1, n_2}(t) + f_{n_1, n_2+1}(t) + f_{n_1, n_2-1}(t) + [\epsilon_{n_1} + \epsilon_{n_2} + F(n_1 + n_2) + \delta_{n_1, n_2} U] f_{n_1, n_2}(t), \quad (4)$$

where we used units of $\hbar = W = e = a = 1$. The above set of equations was solved numerically using a high-order method based on the Taylor expansion of the evolution operator $A(\Delta t)$,

$$A(\Delta t) = \exp(-iH\Delta t) = 1 + \sum_{l=1}^{n_o} \frac{(-iH\Delta t)^l}{l!}, \quad (5)$$

where H is the Hamiltonian. The wave function at time Δt is given by $|\Phi(\Delta t)\rangle = A(\Delta t)|\Phi(t=0)\rangle$. The method can be used recursively to obtain the wave function at time t . The following results were taken by using $\Delta t = 0.05$ and the sum was truncated at $n_o = 20$. This cutoff was sufficient to keep the wave-function norm conservation along the entire time interval considered. We followed the time evolution of an initially Gaussian wave packet of width σ ,

$$\langle n_1 s_1, n_2 s_2 | \Phi(t=0) \rangle = \frac{1}{A(\sigma)} \exp[-(n_1 - n_1^0)^2 / 4\sigma^2] \times \exp[-(n_2 - n_2^0)^2 / 4\sigma^2]. \quad (6)$$

Once Eq. (4) is solved for the initial condition (6), we compute the average centroid's position $X(t)$ and velocity $V(t)$ defined as

$$X(t) = \frac{1}{2} [\langle n_1 \rangle(t) + \langle n_2 \rangle(t)],$$

$$V(t) = -2 \sum_{n_1, n_2} f_{n_1, n_2} [J_{n_1+1, n_2}^* + J_{n_1, n_2+1}^*], \quad (7)$$

where

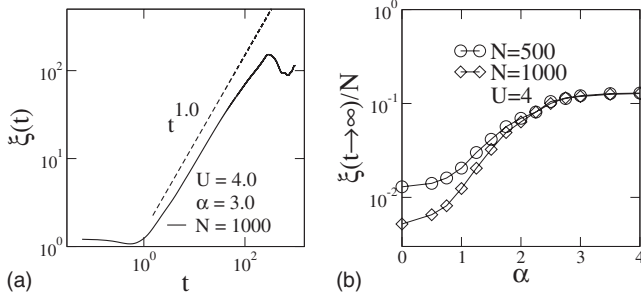


FIG. 1. (a) Spatial extension versus time for $\alpha=3$, $N=1000$ sites, and $U=4$. (b) Scaled long-time spatial extension $\xi(t \rightarrow \infty)/N$ versus the correlation controlling parameter α . Clear signatures of extended states are found at the strong correlation limit ($\alpha > 2$) (ballistic spread followed by a plateau with $\xi \propto N$).

$$\langle n_i \rangle(t) = \sum_{n_1, n_2} (n_i) |f_{n_1, n_2}(t)|^2, \quad i = 1, 2. \quad (8)$$

In addition, to characterize the spacial extension of the two-electron wave packet, we rely on the spacial extension $\xi(t)$ defined as^{36,37}

$$\xi(t) = \sum_{n_1, n_2} \sqrt{\{[n_1(t) - n_1^0]^2 + [n_2(t) - n_2^0]^2\}} |f_{n_1, n_2}(t)|^2. \quad (9)$$

The initial position of the electrons (n_1^0, n_2^0) will be considered to be $(L/2 - d_0, L/2 + d_0)$. The spacial extension $\xi(t)$ is equal to 0 for states with both electrons localized in a single site. It becomes proportional to N when both electrons are uniformly distributed along the chain.^{36,37} This function measures the wave function spread on the $n_1 \times n_2$ plane. The correlated nature of the two-electron dynamics can be numerically probed by computing the two-point correlation function written as

$$\zeta = \langle n_1 n_2 \rangle - \langle n_1 \rangle \langle n_2 \rangle, \quad (10)$$

where $\langle n_1 \rangle$ and $\langle n_2 \rangle$ are the electrons average positions given by Eq. (8) and

$$\langle n_1 n_2 \rangle = \sum_{n_1, n_2} n_1 \cdot n_2 |f_{n_1, n_2}|^2. \quad (11)$$

Further, we analyze the amplitude of the wave function at the initial site, calculating the so-called return probability,^{13,38}

$$R(t) \equiv |f_{n_1^0, n_2^0}(t)|^2. \quad (12)$$

The electrons escaping from their initial positions occur when the return probability $R(t \rightarrow \infty)$ becomes as small as $1/N^2$ as t evolves. Conversely, the return probability saturates at a much larger value for localized as well as for partially trapped wave packets.

In the case of noninteracting electrons, a band of extended states emerges in the strong correlated regime ($\alpha > 2$). In Fig. 1(a) we show data of the spacial extension ξ versus time for $\alpha=3$ and interacting electrons. Calculations were done by solving the two electrons time-dependent Schrödinger equation for $N=1000$ sites with Hubbard interaction $U=4$. Within our numerical precision, ξ shows an initial ballistic electronic spread followed by a plateau that signals the arrival of the

wave packet at the chain borders. In Fig. 1(b), we compute the scaled long-time spacial extension $\xi(t \rightarrow \infty)/N$ versus the correlation parameter α . In this case, we numerically integrate the wave equation until a stationary state can be reached. In the presence of extended states, $\xi(t \rightarrow \infty)$ saturates at a value proportional to N due to the multiple reflections of the wave packet at the chain boundaries. On the other hand, it shall display a slower finite-size scaling when the wave packet is localized on a finite segment of the chain. In agreement with the one-electron case, the collapse of data for $\alpha > 2$ signals the emergence of extended two-electron eigenstates.

To analyze the main effect caused by the electron-electron interaction in the two-electron wave-packet dynamics, we concentrate our attention to the regime of strongly correlated disorder $\alpha > 2$ for which the wave packet spreads over the entire chain in the absence of the electron-electron interaction. In Fig. 2, we report the time evolution of the one-electron wave-packet profile ($|f_n(t)|^2 = \sum_m |f_{n,m}(t)|^2$) computed using $N=1000$, $\alpha=3$, $d_0=0$, $F=0$, (a) $U=0$, (b) $U=4$, and (c) $U=30$. One clearly sees that a finite fraction of the wave packet becomes trapped at the initial position when the Hubbard coupling increases. A more quantitative description is shown in Fig. 3 where the long-time return probability $R(t \rightarrow \infty)$ [Fig. 3(a)] and the long-time electron-electron correlation function $\zeta(t \rightarrow \infty)$ [Fig. 3(b)] are plotted in terms of the Hubbard interaction U . Both quantities increase as the interaction is increased implying in a correlated distribution of the two-electron wave packet. In particular, the long-time correlation function increases linearly in the regime of weak coupling [see inset of Fig. 3(b)]. These results are consistent with the predominant role played by the two-electron bounded states in the regime of strongly correlated electrons.

An uniform external field applied along the chain length promotes the localization of the electronic wave packet. In uncorrelated disordered systems, this localization results in incoherent oscillations of the wave packet around its initial position, with an amplitude that decreases with the field strength. In the absence of disorder, these oscillations become coherent, usually termed as Bloch oscillations. Within a semiclassical approach, the typical frequency of the Bloch oscillations is proportional to the field strength and inversely proportional to the energy bandwidth. It has been shown that the introduction of long-range correlations in the disorder distribution leads to the emergence of a band of extended states⁸ and that the one-electron wave packet displays coherent oscillations in the presence of an external field whose amplitude is proportional to the width of the band of extended states.¹⁶ The build up of coherent oscillations for the case of a two-electron wave packet can be illustrated by phase-space plots of the center-of-mass velocity and position of the two-electron wave packet ($X \times V$), as shown in Fig. 4. Calculations were performed using $N=500$ sites, $U=0.0$ and the initial location of the wave packet $(n_0, m_0) = (N/2, N/2)$. Two representative cases are illustrated: (a) $\alpha=0$ and (b) $\alpha=3$. For both cases, the integration time used was $t=1000$. In Fig. 4(a) one has the typical incoherent oscillations of the electrons wave packet, as expected for uncorrelated disordered systems, reflecting the absence of a typical frequency on the centroid dynamics (see Ref. 16). In Fig. 4(b), the

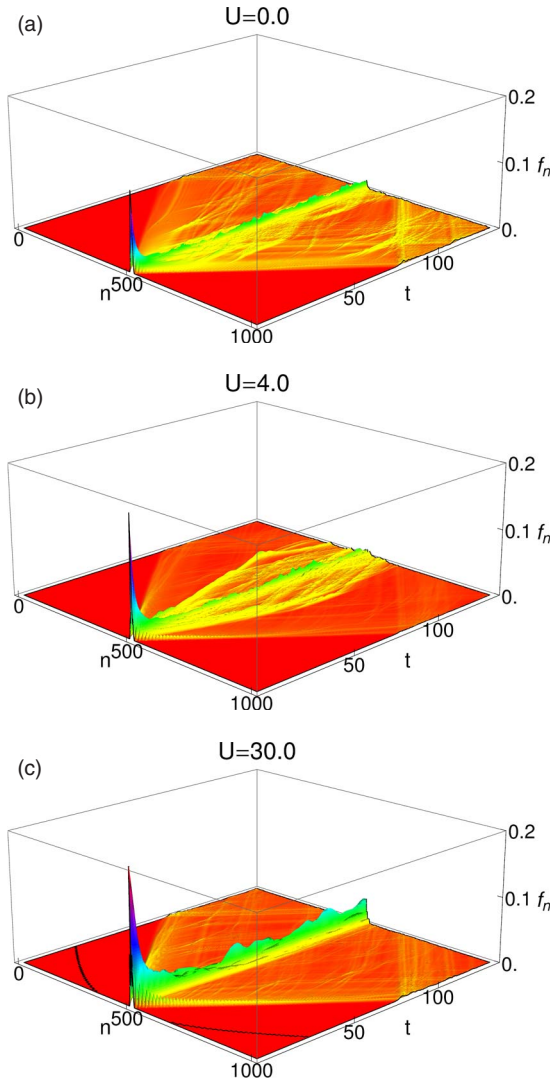


FIG. 2. (Color online) Time evolution of the one-electron wave function $|f_n(t)|^2 = \sum_m |f_{n,m}(t)|^2$ versus t and n computed using $N=1000$, $d_0=0$, $F=0$, $\alpha=3$, (a) $U=0$, (b) $U=4$, and (c) $U=30$. For $U > 0$ a finite fraction of the wave packet remains trapped on the initial site.

phase-space diagram shows coherent oscillations with a slowly varying amplitude. This is a clean signature of Bloch oscillations which are associated with the emergence of ex-

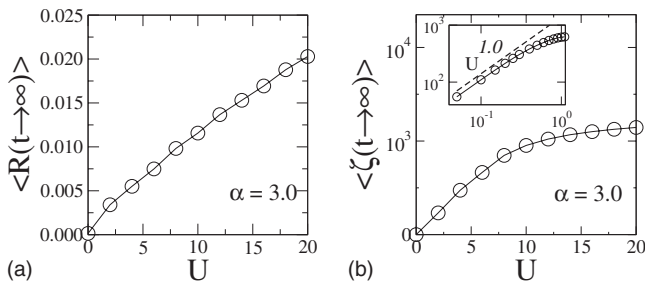


FIG. 3. (a) The long-time return probability $R(t \rightarrow \infty)$ and (b) the long-time correlation function $\zeta(t \rightarrow \infty)$ versus the Hubbard interaction U . The coupling correlates the two electrons and traps a finite portion of the wave packet.

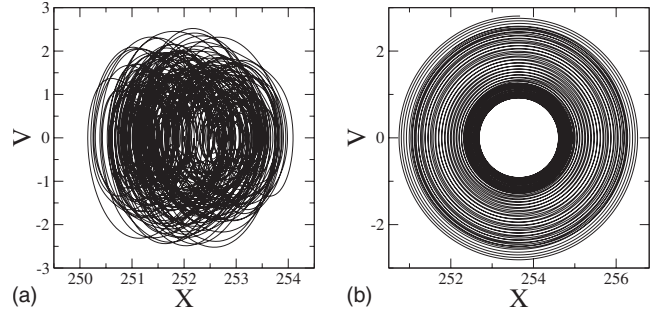


FIG. 4. Phase portraits of the centroid’s velocity vs position for $N=500$ sites, $U=0.0$, $F=0.5$, and the initial location of the wave packet $(n_0, m_0) = (N/2, N/2)$. (a) $\alpha=0$, showing incoherent oscillations. (b) $\alpha=3$, with coherent orbits in phase space indicating Bloch-type oscillations.

tended states in this strongly correlated regime.^{16,39} When the Hubbard coupling is finite, both centroid and velocity display amplitude-modulated envelopes and multifrequency patterns. In Fig. 5, we display the time evolution of the centroid’s velocity computed using $N=500$ sites, $\alpha=3$, and $U=4.0$. The two-electron wave packet reveals a complex oscillatory amplitude-modulated pattern. Its Fourier transform $V(\omega)$ displays a predominant narrow peak close to $\omega=2F$. The modulation in the oscillation pattern observed at finite U is mainly related to the small splitting of the peak at $\omega=F$. Such splitting is on the order of Δ^2/U for large U , where Δ is the width of two-electron crystalline band. It is due to the electron-electron interaction which is also responsible for the emergence of an additional oscillation frequency of the drift velocity of bounded eigenstates.³² The frequency doubling phenomena observed in Fig. 5(b) were established in Ref. 36 for two electrons moving in a 1D pure chain. As the interaction is turned on, the emergence of bounded states correlates the electrons motion.

B. Eigenstates

The numerical solution of the time-dependent Schrödinger equation has shown several signatures of delo-

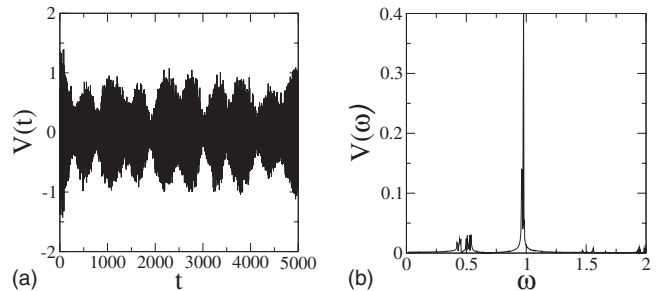


FIG. 5. (a) Time evolution of the centroid’s velocity computed using $N=500$ sites, $\alpha=3$, $F=0.5$, and $U=4.0$. (b) The Fourier spectrum of the velocity. The spectrum exhibits a splitting of the peak at the usual frequency of the one-electron Bloch oscillation $\omega=F$. Such intermediate Hubbard interaction give rises to an oscillatory pattern with a predominant frequency close to $\omega=2F$ due to the correlated motion of the electrons.

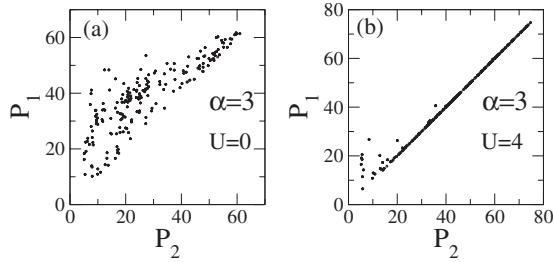


FIG. 6. Participation number associated with each electron $P_1 \times P_2$ for all energy eigenstates near the band center. (a) Without Hubbard coupling: there are two-electron eigenstates for which the electrons have quite distinct participation numbers. (b) For $U=4$: both electrons show approximately the same participation number, except the most localized ones.

calized eigenstates in the long-range correlated 1D model with interacting electrons. In this section, we will apply an exact diagonalization procedure to further explore the particularities of these extended eigenstates. We start by diagonalizing Hamiltonian (1) at zero field and computing the participation number associated with each electron. In our calculations, we followed the usual definition of the participation number^{37,40} [$P(E) = 1 / (\sum_{n_1, n_2} |f_{n_1, n_2}(E)|^4)$] to define the participation number associated to each electron P_i ,

$$P_i(E) = \frac{1}{\sum_{n_i=1}^N |f_{n_i}(E)|^4}, \quad (13)$$

where $|f_{n_i}(E)|^2 = \sum_{n_j} |f_{n_i, n_j}(E)|^2$ is the probability density for a single electron. In general lines, $P_i(E)$ measures the number of sites on which the i th electron is spread in the eigenvector of energy E . In Fig. 6, we show data of P_1 versus P_2 of all states near the band center ($|E| < 0.5$) using $N=120$ sites, $\alpha=3$, (a) $U=0$ and (b) $U=4$. We have labeled the electrons in such a way to have $P_1 > P_2$ for all states, i.e., electron in Eq. (1) was chosen to be the most extended one. It is important to call attention to the fact that extended and localized one-electron eigenstates can coexist within the same energy range. In the case without interaction [Fig. 6(a)], we can even have one electron extended and the other one localized, i.e., $P_1 \gg P_2$ for a given eigenstate. The eigenstates are degenerated and composed of the direct product of one-electron states ($|\phi_{1,2}(E)\rangle = |\phi_1(E_1)\rangle |\phi_2(E_2)\rangle$, with $E = E_1 + E_2$). With the electron-electron interaction turned on ($U=4$), this degeneracy is broken down and the stationary states can no more be written as a direct product. As we can see in Fig. 6(b), the electrons become correlated, with both of them showing approximately the same participation number, except the most localized ones that cannot be efficiently mixed by the electron-electron coupling. In Fig. 7, we plot the most delocalized and most localized participation number within the energy range $|E| < 0.5$ as a function of the chain size. One can clearly see that while the most delocalized state is indeed an extended state in the thermodynamic limit ($P_{\max} \propto N$), the most localized state occupies just a vanishing fraction of the chain ($P_{\min}/N \rightarrow 0$).

Motivated by the coexistence of localized and delocalized states within the same energy range for the two-electron sys-

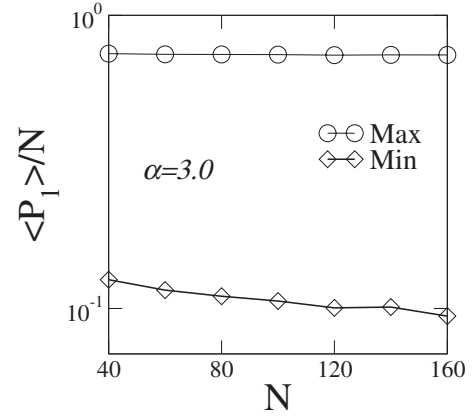


FIG. 7. The maximum and minimum participation numbers associated with a single electron versus N in the energy range around the band center ($-0.5 < E < 0.5$). Data were obtained using $N=40$ up to 160 sites, $\alpha=3$, $U=4$, and averaged over 500 distinct samples. The maximum participation number corresponds to an extended state ($P_{\max} \propto N$) while the minimal one is localized occupying a vanishing fraction of the chain in the thermodynamic limit ($P_{\min}/N \rightarrow 0$).

tem, we analyzed the level spacing statistics near the band center. This may display new features as compared with single electron systems for which extended and localized states usually do not coexist in the same energy range. In one-electron systems, localized states are uncorrelated in energy and distributed following a Poisson law $P(s) = e^{-s}$, where s is the level spacing measured in units of the mean spacing. In contrast, delocalized eigenfunctions repel each other and their level spacing distribution assumes the Wigner form $P(s) \propto s e^{-Cs^2}$.^{41,42} At the Anderson transition a new universal critical statistics intermediate between Wigner and Poisson has been suggested as a consequence of the multifractality of critical wave functions.⁴³ To obtain the level spacing distribution, we used an energy window near the band center ($-0.5, 0.5$). A spectral unfolding procedure was employed to keep the average level spacing equal to unity in each segment of the energy window.⁴³ In Fig. 8, we plot the level spacing distributions computed using $N=120$ sites, $\alpha=3$, $U=0$, $U=2$, and $U=4$. In the absence of electron-electron interaction, the level spacing distribution display a pronounced deltalike singularity at $s=0$. This is associated with the degeneracy of the total energy $E = E_1 + E_2$ with E_1 varying within the single electron energy band. From the total number N_0 of states enclosed in the energy interval considered, the number of degenerated states will be given by the total number of pairs $N_0^2/2$. The remaining states shall follow the usual Poisson distribution. Therefore we expect the level spacing to assume the combined form $P(s) = (1/2)\delta(s) + (1/4)e^{-s/2}$, where s is measured in units of the average level spacing, including the degenerated and nondegenerated ones. The presence of extended states does not affect the distribution because nondegenerated states that are nearest neighbors in energy are seldom a couple of extended states due to their intrinsic level repulsion. The straight line fitting the data for $U=0$ in the inset of Fig. 8 corresponds to the exponential term of the proposed distri-

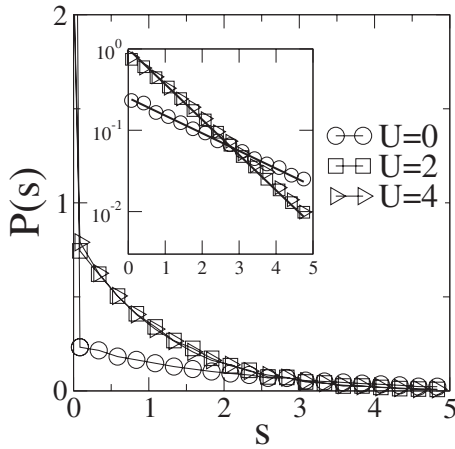


FIG. 8. Level spacing distributions computed using $N=120$ sites, $\alpha=3$, for distinct Hubbard couplings $U=0$, $U=2$, and $U=4$. Even at this strong correlated regime for which delocalized states are present near the band center, the level spacing distributions display a Poisson-type form $P(s) \propto \exp(-As)$. $P(s)$ has a deltalike singularity at $s=0$ for $U=0$, signaling the degeneracy in the energy spectrum. The electron-electron interaction removes the degeneracy and $P(s)$ reassumes the usual Poisson form irrespective to the strength of the Hubbard coupling.

bution. For interacting electrons, the degeneracy is broken and the delta singularity is removed. The distribution recovers its usual Poisson form $P(s)=\exp(-s)$, as shown by the line fitting the data for finite U in the inset of Fig. 8. The small deviation at small s is a finite-size effect. It is important to notice the universality of the level spacing distribution with regard to the interaction strength U .

III. SUMMARY AND CONCLUSIONS

In this work, we studied the problem of two interacting electrons on a 1D lattice with on-site long-range correlated disorder. Long-range correlations were introduced by using a discrete Fourier method which generates an appropriate disorder distribution with spectral density $S(k) \propto 1/k^\alpha$. In the regime of strong correlations ($\alpha > 2$) this model presents a finite-energy range around the band center with extended eigenstates. In this regime, the introduction of an electron-electron coupling leads to the trapping of a finite fraction of the wave packet around its initial position, thus resulting in a

finite return probability and a correlated electronic distribution.

With the electric field F turned on, the motion of the wave packet depicts incoherent oscillations in the weak correlation limit $\alpha < 2$, due to the localized nature of all electronic eigenstates. However, in the strongly correlated regime ($\alpha > 2$) and in the absence of an electron-electron interaction, the wave-packet centroid develops coherent Bloch oscillations whose characteristic frequency is given by $\omega = eFa/\hbar$ according to a semiclassical approach,¹⁶ where e is the electron charge and a is the lattice spacing. For interacting electrons, the wave-packet centroid shows complex Bloch oscillations revealing a multifrequency spectrum. The power spectrum of the centroid velocity trace develops a splitting of the usual peak at $\omega = eFa/\hbar$ and the emergence of a frequency doubled component. Such frequency doubling phenomenon is similar to the one previously reported in Ref. 36 for two electrons moving in a 1D pure chain. It is associated with the emergence of two-electron bounded states. For these components of the wave packet, the coupled electrons effectively behave as a single particle with charge $2e$, thus leading to the frequency doubling of the Bloch oscillations.

Finally, we computed the participation number of the two-electron eigenstates and the level spacing distribution around the center of the energy band in the regime of strong correlations. For noninteracting electrons, the states near the band center are highly degenerated, with localized and extended two-electron states coexisting. This feature contrasts with the usual behavior of single electron systems for which localized and extended states might be separated by mobility edges. Although the degeneracy impacts the level spacing statistics, the presence of extended states is irrelevant, with the distribution function being well described by the superposition of a deltalike peak and a Poissonian decay. The electron-electron interaction correlates the two-electron wave function which reduces the energy levels degeneracy. In this case, the level spacing distribution reassumes its usual pure Poissonian form which has a universal character irrespective to the electron-electron coupling.

ACKNOWLEDGMENTS

This work was partially supported by the Brazilian research agencies CNPq, CAPES, FINEP, Rede Nanobioestruturas, as well as by the Alagoas State research agency FAPEAL.

¹B. Kramer and A. MacKinnon, Rep. Prog. Phys. **56**, 1469 (1993); E. Abrahams, P. W. Anderson, D. C. Licciardello, and T. V. Ramakrishnan, Phys. Rev. Lett. **42**, 673 (1979); for a review see, e.g., I. M. Lifshitz, S. A. Gredeskul, and L. A. Pastur, *Introduction to the Theory of Disordered Systems* (Wiley, New York, 1988).

²B. Huckestein and L. Schweitzer, Phys. Rev. Lett. **72**, 713 (1994).

³R. Ketzmerick, K. Kruse, S. Kraut, and T. Geisel, Phys. Rev.

Lett. **79**, 1959 (1997).

⁴J. C. Flores, J. Phys.: Condens. Matter **1**, 8471 (1989).

⁵D. H. Dunlap, H.-L. Wu, and P. W. Phillips, Phys. Rev. Lett. **65**, 88 (1990); H.-L. Wu and P. W. Phillips, *ibid.* **66**, 1366 (1991); P. W. Phillips and H.-L. Wu, Science **252**, 1805 (1991).

⁶A. Sánchez and F. Domínguez-Adame, J. Phys. A **27**, 3725 (1994); A. Sánchez, E. Maciá, and F. Domínguez-Adame, Phys. Rev. B **49**, 147 (1994).

⁷F. A. B. F. de Moura, M. N. B. Santos, U. L. Fulco, M. L. Lyra,

- E. Lazo, and M. E. Onell, *Eur. Phys. J. B* **36**, 81 (2003); S. S. Albuquerque, F. A. B. F. de Moura, M. L. Lyra, and E. Lazo, *Phys. Lett. A* **355**, 468 (2006).
- ⁸F. A. B. F. de Moura and M. L. Lyra, *Phys. Rev. Lett.* **81**, 3735 (1998); *Physica A* **266**, 465 (1999).
- ⁹F. M. Izrailev and A. A. Krokhin, *Phys. Rev. Lett.* **82**, 4062 (1999); F. M. Izrailev, A. A. Krokhin, and S. E. Ulloa, *Phys. Rev. B* **63**, 041102(R) (2001).
- ¹⁰G. P. Zhang and S.-J. Xiong, *Eur. Phys. J. B* **29**, 491 (2002).
- ¹¹H. Shima, T. Nomura, and T. Nakayama, *Phys. Rev. B* **70**, 075116 (2004).
- ¹²G. Schubert, A. Weiße, and H. Fehske, *Physica B* **359-361**, 801 (2005).
- ¹³F. A. B. F. de Moura, M. D. Coutinho-Filho, E. P. Raposo, and M. L. Lyra, *Europhys. Lett.* **66**, 585 (2004).
- ¹⁴V. Bellani, E. Diez, R. Hey, L. Toni, L. Tarricone, G. B. Parravicini, F. Domínguez-Adame, and R. Gomez-Alcala, *Phys. Rev. Lett.* **82**, 2159 (1999); V. Bellani, E. Diez, A. Parisini, L. Tarricone, R. Hey, G. B. Parravicini, and F. Domínguez-Adame, *Physica E (Amsterdam)* **7**, 823 (2000).
- ¹⁵U. Kuhl, F. M. Izrailev, A. Krokhin, and H. J. Stöckmann, *Appl. Phys. Lett.* **77**, 633 (2000).
- ¹⁶F. Domínguez-Adame, V. A. Malyshev, F. A. B. F. de Moura, and M. L. Lyra, *Phys. Rev. Lett.* **91**, 197402 (2003).
- ¹⁷F. A. B. F. de Moura, M. L. Lyra, F. Domínguez-Adame, and V. A. Malyshev, *J. Phys.: Condens. Matter* **19**, 056204 (2007).
- ¹⁸D. L. Shepelyansky, *Phys. Rev. Lett.* **73**, 2607 (1994).
- ¹⁹Y. Imry, *Europhys. Lett.* **30**, 405 (1995).
- ²⁰K. Frahm, A. Muller-Goeling, J.-L. Pichard, and D. Weinmann, *Europhys. Lett.* **31**, 169 (1995).
- ²¹P. Jacquod and D. L. Shepelyansky, *Phys. Rev. Lett.* **75**, 3501 (1995).
- ²²Y. V. Fyodorov and A. D. Mirlin, *Phys. Rev. B* **52**, R11580 (1995).
- ²³K. Frahm, A. Muller-Groeling, and J.-L. Pichard, *Phys. Rev. Lett.* **76**, 1509 (1996).
- ²⁴M. Leadbeater, R. A. Romer, and M. Schreiber, *Eur. Phys. J. B* **8**, 643 (1999).
- ²⁵K. Frahm, *Eur. Phys. J. B* **10**, 371 (1999).
- ²⁶O. Halfpap, *Ann. Phys.* **10**, 623 (2001).
- ²⁷A. Eilmès, R. A. Romer, and M. Schreiber, *Eur. Phys. J. B* **23**, 229 (2001).
- ²⁸A. Eilmès, U. Grimm, R. A. Romer, and M. Schreiber, *Eur. Phys. J. B* **8**, 547 (1999).
- ²⁹R. A. Römer and M. Schreiber, *Phys. Rev. Lett.* **78**, 515 (1997).
- ³⁰S. N. Evangelou, S.-J. Xiong, and E. N. Economou, *Phys. Rev. B* **54**, 8469 (1996).
- ³¹S. N. Evangelou and D. E. Katsanos, *Phys. Rev. B* **56**, 12797 (1997).
- ³²F. Claro, J. F. Weisz, and S. Curilef, *Phys. Rev. B* **67**, 193101 (2003).
- ³³A. Buchleitner and A. R. Kolovsky, *Phys. Rev. Lett.* **91**, 253002 (2003).
- ³⁴J. K. Freericks, V. M. Turkowski, and V. Zlatić, *Phys. Rev. Lett.* **97**, 266408 (2006).
- ³⁵G. Xianlong, M. Polini, M. P. Tosi, V. L. Campo, K. Capelle, and M. Rigol, *Phys. Rev. B* **73**, 165120 (2006).
- ³⁶W. S. Dias, E. M. Nascimento, M. L. Lyra, and F. A. B. F. de Moura, *Phys. Rev. B* **76**, 155124 (2007).
- ³⁷W. S. Dias, E. M. Nascimento, F. A. B. F. de Moura, and M. L. Lyra, *J. Magn. Magn. Mater.* **321**, 2304 (2009).
- ³⁸H. N. Nazareno and P. E. de Brito, *Phys. Rev. B* **60**, 4629 (1999).
- ³⁹F. A. B. F. de Moura, L. P. Viana, M. L. Lyra, V. A. Malyshev, and F. Domínguez-Adame, *Phys. Lett. A* **372**, 6694 (2008).
- ⁴⁰I. F. dos Santos, F. A. B. F. de Moura, M. L. Lyra, and M. D. Coutinho-Filho, *J. Phys.: Condens. Matter* **19**, 476213 (2007).
- ⁴¹M. L. Mehta, *Random Matrices* (Academic, Boston, 1991).
- ⁴²R. P. A. Lima, H. R. da Cruz, J. C. Cressoni, and M. L. Lyra, *Phys. Rev. B* **69**, 165117 (2004).
- ⁴³S. N. Evangelou and D. E. Katsanos, *J. Stat. Phys.* **85**, 525 (1996).